STABILITY INDEX CONSIDERING SLAB STRENGTH

Shinji Ikeda[1]*, Takafumi Katsushima[2], Yasuhiko Ito[1], Yukari Takeuchi[3], Tomoyuki Noro[1]
[1]Public Works Research Institute, Snow Avalanche and Landslide Research Center
[2]Toyama National College of Technology
[3]Tohkamachi Experimental Station, Forestry and Forest Products Research Institute

ABSTRACT: When a slab avalanche is triggered, the weak layer and all sides of the slab (crown, flank, and stauchwall) are fractured. Wet slab avalanches frequently involve thick, strong slabs. At present, the stability index is defined as the ratio of the strength of the weak layer to the stress induced by the slab weight; we think that this index underestimates stability, especially in warm heavy-snow regions such as those in central Japan. For more realistic stability evaluation of wet slab avalanches, we propose a stability index that considers the slab strength.
To estimate the slab strength, slabs are classified into three size-based groups: 10 m × 10 m, 50 m × 50 m, 100 m × 100 m. Furthermore, the slab states are classified into four types depending on the effective part of the slab acting as support: wcfs (weak layer, crown, flank, and stauchwall), wcf (weak layer, crown, and flank),wfs (weak layer, flank, and stauchwall), and wf (weak layer and flank). The results of our test calculation suggest that the slab strength should not be disregarded when evaluating stability, especially for small, high-density slabs. We believe that the proposed stability index will be useful in avalanche safety operations because it can lower the false alarm rate by considering the slab size and effective part of the slab.

1. INTRODUCTION

As an index for evaluating avalanche danger = stability of snow on a slope, a stability index (SI) has been proposed and defined as a ratio of the drive force in the direction of the slope initiated by shear strength of the weak layer to the stress induced by the slab weight (e.g., Roch, 1966; Perla, 1977) :

$$SI = \sigma_w / W \cdot \sin\theta\cos\theta \qquad (1)$$

σ_w: shear strength of the weak layer ($N \cdot m^{-2}$)
W: Snow weight per unit of horizontal area ($N \cdot m^{-2}$)
θ: Slope angle (°)

In many cases, the shear frame index (SFI) is used to denote the strength of the weak layer upon calculation of *SI* (Roch, 1966; Perla, 1977). *SFI* is the shear strength of a weak layer and is measured by using a shear frame with a constant effective shear area divided by the effective shear area. Methods to determine the *SFI* from snow density and hardness have been proposed in recent years to make the calculation of *SFI* even easier (Yamanoi et al., 2004). However, *SFI* is different from the actual shear strength, because it is measured on deformation rate different from on an avalanche initiation, and there is the impact of the size of the shear frame. *SI* also has no mechanism to consider the fracture propagation, and the index has been criticized for being incomplete in explaining the actual occurrence of an avalanche (Schweizer et al., 2003). However, its applicability has been widely recognized as one of the indexes that best estimates the danger of occurrence of an avalanche to this day, and it has been used in situations such as road management (Jamieson, 1995).

Studies on predicting avalanches using a snowpack model (e.g., Lehning et al., 2002; Hirashima et al., 2008) have often employed *SI* as an output of stability. However, such studies focused primarily on modeling the snow layer structure and reproducibility of the snow grain shapes and failed to discuss the validity of the calculation method for snow stability.

As shown in figure 1, avalanches involve not only fracture at the weak layer under the slab but also in all four sides of a slab (crown, flank, and stauchwall). The strength of the slab is expected to affect its stability, especially for heavy snow and warm region where high density strong snow layers consisted by Rounded Grains and Melt Forms are prominent, and during the snowmelt period. Therefore, we propose a new form of snow stability that takes slab strength into account and discuss its usability in order to estimate snow stability more accurately.

*Corresponding and presenting author: Ikeda H.
2-6-8, Nishiki-cho, Myoko-City, Niigata-Pref, 944-0051, Japan
Phone: +81-255-72-4131
Fax: +81-255-72-9629
e-mail: s-ikeda55@pwri.go.jp

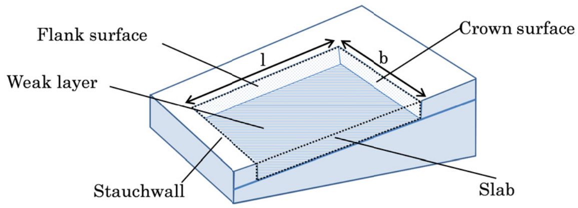

Fig. 1 Snow fracture in avalanches initiation

2. METHODS

This paper proposes a method of stability that takes slab strength into account. The proposed method of stability was used to calculate a new *SI* for an example observed snow profile and for one winter period, and these results of calculations are compared with conventional *SI*. We used these calculation results to evaluate the usability of the new stability method.

2.1 Stability considering slab strength

We defined the unstable condition as "drive force > strength of the weak layer + slab strength" and assumed fracture to be in the four sides of the slab: the crown (tensile fracture), flank (shear fracture), and stauchwall (compressive fracture). For this unstable condition, fracture was assumed to occur in both the weak layer and slab same time an avalanche occurs. Therefore, stability was defined as the ratio of the sum of the strengths of the weak layer and slab to the stress created by the snow weight in the direction of the slope. First, the strength in the four sides of the slab was added to equation (1), which calculates *SI* for the proposed equation (2). Based on this equation, equations (3)–(5) are proposed to consider the state of the slope, such as the effectiveness of the slab's bearing power as determined by the landscape form, appearance of cracks in the slab, and disappearance of the bearing power due to the removal of snow (table 1). The dimensions of the slab are needed to calculate stability using equations (2)–(5). For this study, three slab sizes were assumed for b (slab width) × l (slab length): 10 m × 10 m, 50 m × 50 m, and 100 m × 100 m.

$$SIwcfs = \{bl\sigma_w + bh(\sigma_c + \sigma_s) + 2lh\sigma_f\} / (blW \cdot \sin\theta \cos\theta) \quad (2)$$

$$SIwcf = (bl\sigma_w + bh\sigma_c + 2lh\sigma_f) / (blW \cdot \sin\theta \cos\theta) \quad (3)$$

$$SIwfs = (bl\sigma_w + bh\sigma_s + 2lh\sigma_f) / (blW \cdot \sin\theta \cos\theta) \quad (4)$$

$$SIwf = (bl\sigma_w + 2lh\sigma_f) / (blW \cdot \sin\theta \cos\theta) \quad (5)$$

b: Slab width (m)
l: Slab length (m)
h: Slab thickness (m)
σ_c: Tensile strength of the crown ($N \cdot m^{-2}$)
σ_f: Shear strength of the flank ($N \cdot m^{-2}$)
σ_s: Compressive strength of the stauchwall ($N \cdot m^{-2}$)

Table. 1 Each stability and the assumed slope state

Stability	Assumed slope state	Considered strength	Eq.
SI	Conventional stability	Only the strength of the weak layer is considered	(1)
SIwcfs	All four slab supports are effective	Weak layer, crown, flank (L & R), and stauchwall	(2)
SIwcf	Support from stauchwall is not available due to landscape forms and snow removal	Weak layer, crown, flank (L & R)	(3)
SIwfs	Support from crown is not available due to cracks	Weak layer, stauchwall, flank (L & R)	(4)
SIwf	Support from crown and stauchwall is not available	Weak layer, flank (L & R)	(5)

2.2 Test calculation for an example observed snow profile

Data for the stability calculation were taken from observations at the Tohkamachi Experimental Station, Forestry and Forest Products Research Institute (37°08′ N, 138°46′ E, 200 m a.s.l.). The observed parameters were the snow layer structure, snow grain shapes, grain size, snow temperature, density, water equivalent, and push-pull hardness (Takeuchi et al., 1998). The data were from a snowmelt period during which all layers consisted of a high-density Melt Forms and fragile parts existed at the bottom and middle parts (approximately 100 cm height) (figure 2). Since the slab strength was higher than the snow layers containing the Precipitation particles or the Decomposing precipitation particles in midwinter, the impact of slab strength on slab stability was expected to be greater.

2.3 Test calculation for one winter period

Snowpack for the 2011–2012 winter period at the Tohkamachi Experimental Station, Forestry and Forest Products Research Institute was simulated using a snowpack model and meteorological data. The calculated values were the layer structure, layer thickness, density, grain size, and water equivalent of each layer at hourly increments for the entire winter period.

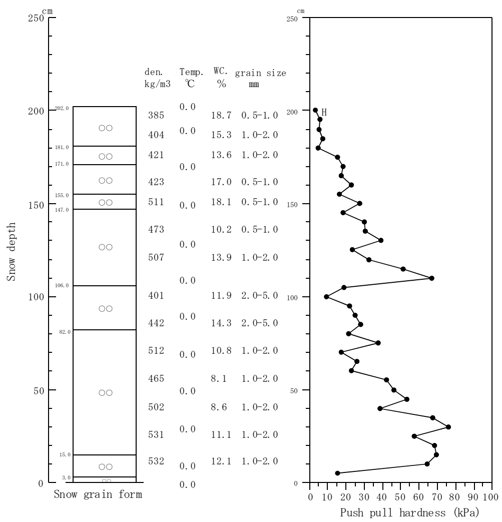

Fig. 2 Observation data for snow profile used to calculate stability
(The Tohkamachi Experimental Station, Forestry and Forest Products Research Institute, March 24, 2005)

The average maximum annual snow depth at the site was over 2 m, but the average temperature was warm at -0.3 ℃ during January and 0 ℃ during February; the snow was typically moist throughout the winter (Yamanoi et al., 2000). We used the snowpack model developed by Katsushima et al. (2009), which considers vertical water channels, but the equation for the water retention curve was changed to that proposed by Yamaguchi et al. (2012) for calculation. Since the permeability for the ground varies greatly by location, the value was set to that of the bottom layer of the snow; infiltration of water from the bottom snow layer to the ground was treated as continuous. Thus, water saturated layer was avoided at the boundary between the snow and ground, which in turn may have caused the water equivalent at the bottom layer of the snow to be underestimated. As a result, the stability of the full depth avalanche may be overestimated, but the surface avalanche is appropriately simulated. The meteorological data used were for the temperature, humidity, precipitation, solar radiation (upward and downward), and radiation budget.

2.4 <u>*Calculation of snow strength and slope angle*</u>

σ_w and σ_f were calculated from the push-pull hardness using the same method as Yamanoi et al. (2004) for test calculations of the observed data and from the snow density and water equivalent using the same method as Yamanoi and Endo (2002) for test calculations on one winter period.

σ_c was calculated from the shear strength using the tensile strength and shear strength ratio of 27.3:4.2, which was determined by Keeler and Weeks (1968) for dry snow. σ_s was assumed to be the same as σ_c since there is no great difference between the compressive and tensile strengths of low-density snow (Maeno and Kuroda, 1986). The calculated results for *SIwcf* and *SIwfs* yielded the same value; hence, their results are shown from here onwards as *SIwcf*(*SIwfs*) instead of being listed individually.

Slope angle θ was assumed to be 40° from the peak in frequency of avalanche occurrence (McClung and Schaerer, 2006).

3. RESULTS AND DISCUSSION

3.1 <u>*Results of test calculation for snow profile observation*</u>

Figure 3 shows each calculated stability for a slab size of 10 m × 10 m. *SI* focusing on the fragile places at the bottom and middle (100 cm height) was 0.8 and 0.9, respectively, and the drive force exceeded the strength. On the other hand, *SI* at the bottom and middle for *SIwcfs* was 6.3 and 4.8, *SIwcf*(*SIwfs*) was 3.9 and 3.1, and *SIwf* was 1.5 and 1.4, respectively; the strength exceeded the drive force.

SIwcfs at the bottom for *bl* = 50 m × 50 m and 100 m × 100 m was 1.8 and 1.3, respectively, and *SIwcfs* in the middle was 1.6 and 1.2, respectively; the strength exceeded the drive force in both places (figure 4).

Table 2 shows each calculated stability in the middle and at the bottom of the snowpack. Stability differed greatly based on whether or not the slab strength was considered; this implies that the slab strength is a factor that cannot be ignored during estimation of the snow stability. However, in cases where the upper and lower strengths are not effective (*SIwf*) or in larger cases with slab sizes of 50 m × 50 m and 100 m × 100 m, changes in stability through the inclusion of slab strength were small. The impact of slab strength on stability large depends on the slope size and state of the slope (effectiveness of the upper and lower strengths of the slab). Additionally, this case study used a snow layer in which the entire layer consisted of Melt Forms, so the overall snow density and slab strength were high. The impact of slab strength on slab stability is thought to be lower for snow layers in which new or Rounded Grains makes up the snow structure.

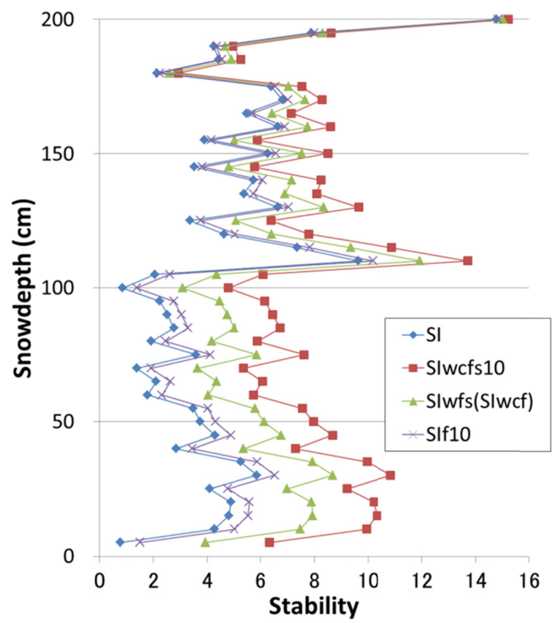

Fig. 3 Slab stability for a slab size of 10 × 10 m *SIwcfs, SIwcf*(*SIwfs*), *SIwf*

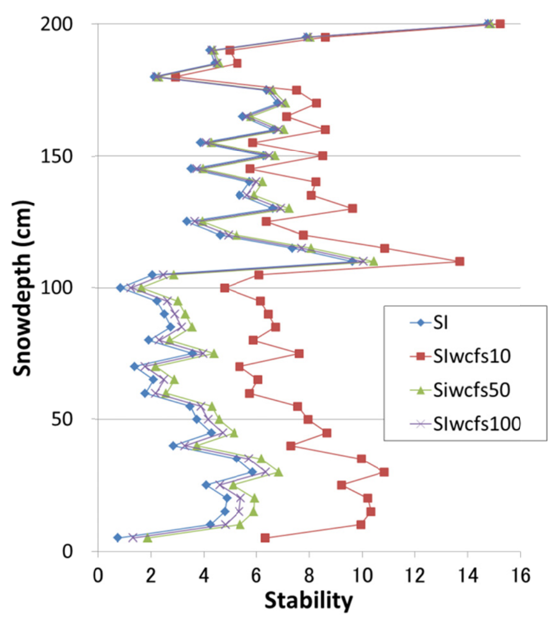

Fig. 4 Stability for each slab size (*SIwcfs*)

Table 2 Calculation results for all stabilities

	Slope size	*SI*	*SIwcfs*	*SIwcf* (*SIwfs*)	*SIwf*
Middle	10 m × 10 m	0.9	4.8	3.1	1.4
	50 m × 50 m	0.9	1.6	1.3	1.0
	100 m × 100 m	0.9	1.2	1.1	0.9
Bottom	10 m × 10 m	0.8	6.3	3.9	1.5
	50 m × 50 m	0.8	1.8	1.4	0.9
	100 m × 100 m	0.8	1.3	1.1	0.8

3.2 Results of test calculation for one winter period

Figure 5 shows some examples of each calculated SI (conventional stability), *SIwcfs*100 (slab size of 100 m × 100 m where support is effective from all four slab sides), *SIwcfs*50 (slab size of 50 m × 50 m where support is effective from all four slab sides), *SIwcfs*10 (slab size of 10 m × 10 m where support is effective from all four slab sides), *SIwcf*10 (slab size 10 m × 10 m where support from the crown or flank and stauchwall of the slab is effective), and *SIwf*10 (slab size of 10 m × 10 m where flank support is effective). Table 3 shows the time of occurrence of an unstable state for each form of stability. Table 3 also shows three cases of the time passed to reach instability, defined as the form of stability for which the bearing power is less than the drive force: stability < 1, stability < 1.5, and stability < 4.0 (Roch, 1966; Perla, 1977). The table also shows their respective ratios (%) against a lingering snow period. There was no great difference compared to conventional *SI* when the slab size was 100 m × 100 m, but the difference became more significant as the slab size became smaller. For example, when the standard of instability was defined as stability < 1.5, the time for the slab to become unstable was *SI*: 1377 h (43% of the lingering snow period),

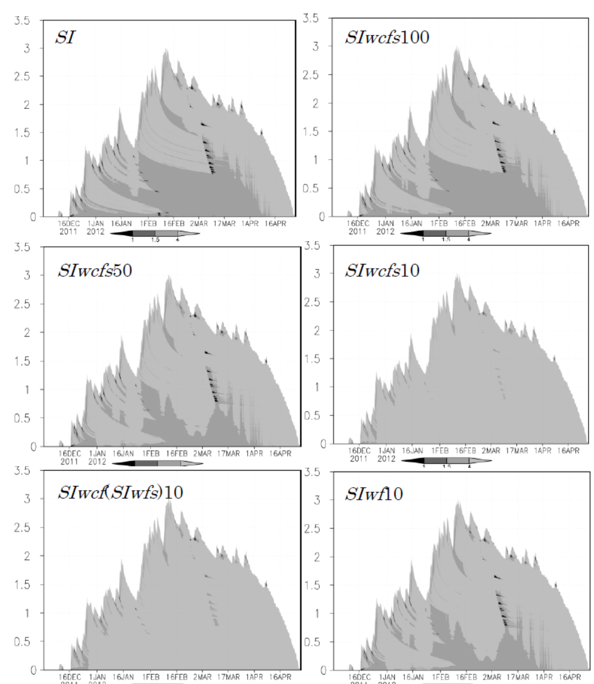

Fig. 5 2011–2012 example of the calculated stability in winter
*Expressed in four stages: less than 1, under 1.5, under 4.0, and over 4.0

Table 3 Time of occurrence of an unstable state for each form of stability

	<1.0		<1.5		<4.0	
	h	%	h	%	h	%
SI	817	26	1377	43	2869	90
SIwcfs100	688	22	1135	36	2819	88
SIwcfs50	594	19	993	31	2745	86
SIwcfs10	54	2	305	10	1908	60
SIwcf(*SIwfs10*)	143	4	569	18	2038	64
SIwf10	590	19	991	31	2743	86

*SIwcfs*100: 1135 h (36%), *SIwcfs*50: 993 h (31%), and *SIwcfs*10: 305 h (10%).On the other hand, for *SIwcf*(*SIwfs*10) where the slab size was 10 m × 10 m but the slab lacked support from either the crown or stauchwall, the time for the slab to reach instability was 569 h (18%). For *SIwf*10, where only the flank support is effective, the time for the slab to reach instability was 991 h (31%). Variances in these results revealed that taking the effectiveness of the bearing power of the slab into account greatly affects the calculation results for stability.

Figure 6 shows the transition in minimum value for *SI* and *SIwcfs*10 (the value for the point in all snow layers with the lowest stability at each point in time). The figure reveals that the overall stability was not simply rated higher for *SIwcfs*10 compared to *SI* but sometimes decreases rapidly; this suggests that *SIwcs*10 accurately captures the state of snow and is quite accurate at reflecting unstable states.

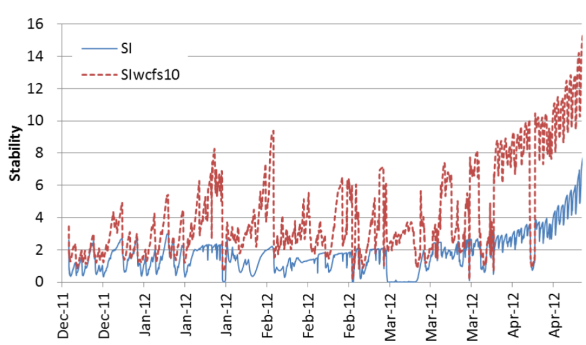

Fig. 6 Transition of minimum values for *SI* and *SIwcfs*10

4. CONCLUSION

The following four stabilities were proposed as a new form of stability that takes slab strength into account:
Siwcfs: Support from all four sides of the slab is effective
Siwcf: Support from the crown and the flank are effective
Siwfs: Support from the flank and the stauchwall are effective
Siwf: Support from the flank is effective

Upon conducting a test calculation for an actual observed snow profile and one winter period and comparing the results with the conventional stability index *SI*, the slab strength was shown to be a factor that cannot be ignored when estimating the stability of snow, although the stability also depends on the size of the slope and state of the slab support. The impact of slab strength is greater on slopes with a smaller scale, especially during the snowmelt period as the snow density is generally higher than the midwinter. Therefore, the stability proposed in this paper is effective at assessing the danger of avalanches on smaller slopes for road management and behind residences.

The proposed snow stability is able to consider the effectiveness of the bearing power of the slab due to the landscape form, cracking conditions on the slab surface, and loss of bearing power by snow removal; thus, the stability can be calculated in more detail and in correspondence with daily inspections of a slope.

The proposed stability may also be able to lessen instances of the false alarm rate in which stable snow is assessed as unstable and calculate stability more accurately than before.

Finally, the new stability focuses on the strength of the weak layer as well as the strengths of multiple layers above the weak layer; thus, it utilizes the output from a multi-layer snowpack model more effectively.

On the other hand, this study used the ratio of tensile and shear strength proposed by Keeler and Weeks (1968) to calculate the slab tensile strength σ_c, but there have been reports of observations where the tensile strength was less than the shear strength of fragile materials, including snow (Podolskiy, 2010). Because the impact of the slab strength on stability varies greatly based on how tensile strength is derived, future studies need to evaluate the tensile strength for various snow qualities, including wet snow.

In addition, while the new stability can decrease the false alarm rate by considering slab strength, which ultimately estimates the stability to be larger than conventional *SI*, the new stability may also overestimate and assess unstable snow as stable. Therefore, the proposed form of stability needs to be tested against actual avalanche cases to establish its validity and an appropriate threshold for its use.

Finally, a slab not only develops a drive force through its weight and strength but also from shrinking of the slab itself. Future studies need to address this.

REFERENCES

Hirashima, H., Nishimura, K., Yamaguchi, S., Sato, A., and Lehning, M., 2008. Avalanche forecasting in a heavy snowfall area using the snowpack model. Cold Regions Science Technology 51, 191-203.

Jamieson, J.B., 1995. Avalanche prediction for persistent snow slabs. Ph.D. Thesis, Dept. of Civil Engineering, University of Calgary, Canada.

Katsushima, T., Kumakura, T., Takeuchi, Y., 2009. A multiple snow layer model including a parameterization of vertical water channel process in snowpack. Cold Regions Science Technology 59(2-3), 143-151.

C.M. Keeler, W.F. Weeks, 1968. Investigations into the mechanical properties of alpine snow-packs. Journal of Glaciology 7(50), 253-271.

Lehning M., P.B. Bartelt, R.L. Brown, C. Fierz, P. Satyawali, 2002: A physical SNOWPACK model for the Swiss avalanche warning services part II: Snow microstructure. Cold Reg. Sci. Technol. 35, 147-167.

Maeno, K., Kuroda, T., 1986. Structure and Physical Properties of Snow and Ice (Fundamental Courses on Snow and Ice vol. 1), Kokon Shoin, 209 pp. (in Japanese).

McClung, D. and Schaerer, P., 2006. The Avalanche Handbook. The Mountaineers Books, Seattle, WA. pp. 271.

Podolskiy, E.A., 2010. Experimental studies on earthquake-induced snow avalanches. Ph.D. Thesis, Department of Earth and Environmental Sciences, Graduate School of Environmental Studies, Nagoya University, 173 pp.

Perla, R., 1977. Slab avalanche measurements. Can. Geotech. J. 14(2), 206-213.

Roch, A., 1966: Les variations de la resistance de la neige. Proceedings of the International Symposium on Scientific Aspects of Snow Avalanches, IAHS Publ., No. 69, 86-99.

Schweizer, J., Jamieson, J.B. and Schneebeli, M., 2003. Snow avalanche formation, Rev. Geophys. 41(4), 1016-1041.

Takeuchi, Y., Nohguchi, Y., Kawashima, K., and Izumi, K., 1998. Measurement of snow hardness distribution. Annals of Glaciology 26, 27-30.

Yamaguchi, S., Watanabe, K., Katsushima, T., Sato, A., Kumakura, T., 2012. Dependence of the water retention curve of snow on snow characteristics (In press).

Yamanoi, K., Endo, Y., Kominami, Y., Niwano, S., Ohzeki, Y., 2000. Meteorological statistics during the past 80 years in Tohkamachi city, Niigata (1918–1997). Bull. For. For. Prod. Res. Inst. 377, 61-99 (in Japanese, with English abstract).

Yamanoi, K., Endo, Y., 2002. Dependence of shear strength of snow cover on density and water content. Seppyo. 64 (4), 443–451 (in Japanese with English Abstruct).

Yamanoi, K., Takeuchi, Y., Murakami, S., 2004. Evaluation of snow stability index by using a digital push-gauge. Seppyo. 66 (6), 669-676 (in Japanese with English abstract).